Proton motive function of the terminal antiporter-like subunit in respiratory complex I

Djurabekova, Amina

2020-07-01

Djurabekova , A , Haapanen , O & Sharma , V 2020 , ' Proton motive function of the terminal antiporter-like subunit in respiratory complex I ' , Biochimica et Biophysica Acta. Bioenergetics , vol. 1861 , no. 7 , 148185 . https://doi.org/10.1016/j.bbabio.2020.148185

http://hdl.handle.net/10138/316688
https://doi.org/10.1016/j.bbabio.2020.148185

BBA - Bioenergetics 1861 (2020) 148185

Contents lists available at ScienceDirect

BBA - Bioenergetics

journal homepage: www.elsevier.com/locate/bbabio

Proton motive function of the terminal antiporter-like subunit in respiratory complex I

Amina Djurabekova[a,1], Outi Haapanen[a,1], Vivek Sharma[a,b,*]

[a] Department of Physics, University of Helsinki, Helsinki, Finland
[b] Institute of Biotechnology, University of Helsinki, Helsinki, Finland

ARTICLE INFO

Keywords:
Mitochondria
Redox reactions
Proton transfer
Cell respiration

ABSTRACT

In the aerobic respiratory chains of many organisms, complex I functions as the first electron input. By reducing ubiquinone (Q) to ubiquinol, it catalyzes the translocation of protons across the membrane as far as ~200 Å from the site of redox reactions. Despite significant amount of structural and biochemical data, the details of redox coupled proton pumping in complex I are poorly understood. In particular, the proton transfer pathways are extremely difficult to characterize with the current structural and biochemical techniques. Here, we applied multiscale computational approaches to identify the proton transfer paths in the terminal antiporter-like subunit of complex I. Data from combined classical and quantum chemical simulations reveal for the first time structural elements that are exclusive to the subunit, and enables the enzyme to achieve coupling between the spatially separated Q redox reactions and proton pumping. By studying long time scale protonation and hydration dependent conformational dynamics of key amino acid residues, we provide novel insights into the proton pumping mechanism of complex I.

1. Introduction

Respiratory complex I is a large membrane-bound enzyme that converts ubiquinone (Q) to ubiquinol upon electron transfer from NADH oxidation [1–3]. This exergonic redox reaction is responsible for the pumping of protons across the membrane to establish a proton electrochemical gradient, which propels ATP synthesis. The most remarkable aspect of complex I is the long-range (~20 nm) coupling between the Q reduction and proton pumping (Fig. 1A), the nature and molecular mechanism of which remains poorly known. A number of high-resolution X-ray and cryo EM structures of complex I have been solved [2], and together with biochemical and spectroscopic data, they have significantly enhanced our understanding. It is generally considered that the reduction of Q by terminal FeS cluster N2 (and reactions beyond it) drives the pumping of protons [4–6], a notion also supported by high-resolution structural data [7,8]. An array of charged residues connects the Q binding site near N2 center to the first putative proton channel in subunits Nqo10/11 (Fig. 1B). Due to lower resolution of structural data, water molecules have not been identified in these key areas of the protein, which may be important in driving Grotthuss-like proton transfer through H-bonded arrays of water molecules [9]. Instead, classical atomistic molecular dynamics (MD) simulations have identified a key role of water molecules and protein dynamics in coupling the Q redox reactions to the nearest proton pumping route [10]. Computer simulations have also provided dynamical insights into the hydrated networks of the antiporter-like subunits (Nqo12-14) that may be used to pump protons from the N-side to the P-side of the membrane [11,12] (Fig. 1A). In the three antiporter-like subunits, the proton uptake routes form in the middle of the subunits by residues from TM helices 7 and 8 [10,13]. In earlier simulation studies, the proton pathways from the N-side were found comparable between the two antiporter-like subunits Nqo13 and Nqo14 [10]. However, in the distant Nqo12 subunit, a similar hydration was less apparent, which is somewhat expected because of the distinct sequence differences between the Nqo12 and Nqo13/14 subunits. For instance, the functionally important lysine (Lys235 and Lys216 in Nqo13 and Nqo14, respectively) from helix 8 is not conserved in the Nqo12 subunit. Instead, Lys329 from helix 11 is conserved, which however is not found in the Nqo13/14 subunits (Fig. 1C and D). This striking difference is complemented by a highly conserved residue His241 from helix 8 in Nqo12, which is also not found in the two other antiporter-like subunits (Fig. 1C and D). Moreover, the two residues His211 and His218 of Nqo13, which were found to be important based on MD simulation studies [10,13] and, which are analogous to His193 and Tyr200 in Nqo14, are replaced by

* Corresponding author at: Department of Physics, University of Helsinki, Helsinki, Finland.
E-mail address: vivek.sharma@helsinki.fi (V. Sharma).
[1] Equal contribution.

https://doi.org/10.1016/j.bbabio.2020.148185
Received 15 September 2019; Received in revised form 15 January 2020; Accepted 9 March 2020

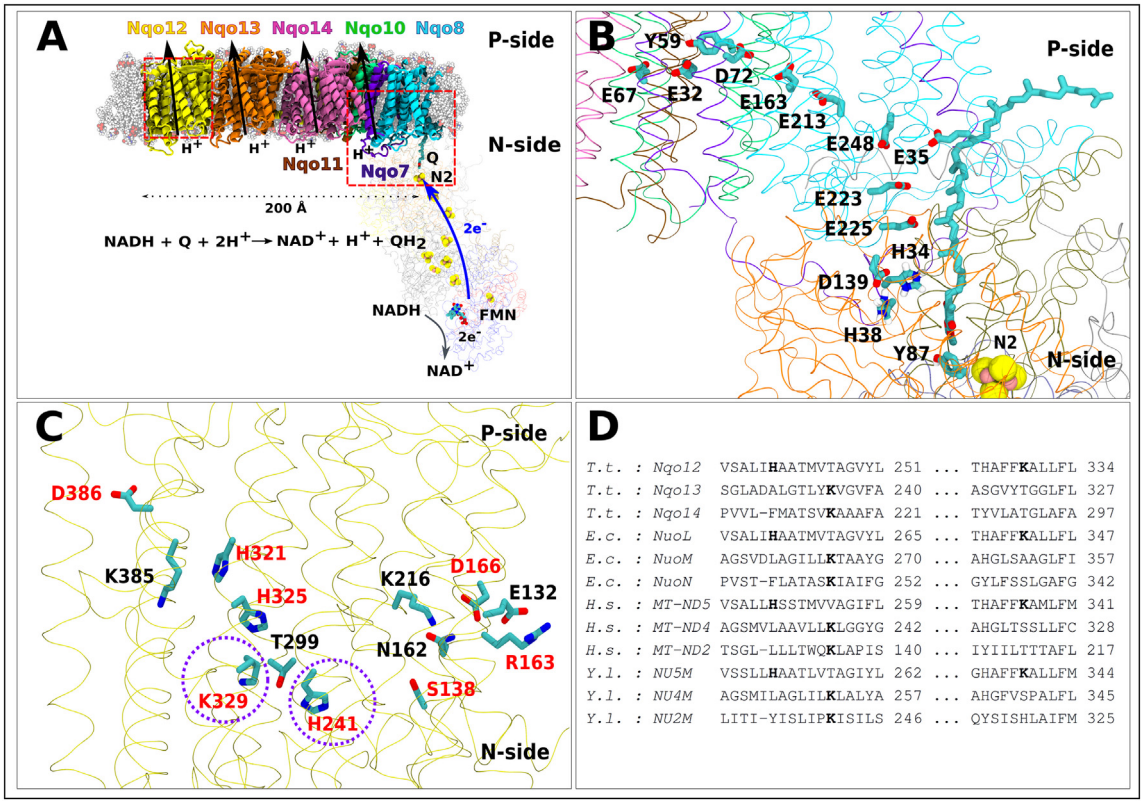

Fig. 1. (A) Respiratory Complex I from *Thermus thermophilus* (PDB id 4HEA) embedded in POPC lipid bilayer. The hydrophilic domain is shown in thin ribbons and membrane domain in thick ribbons with subunit-based coloring. A modeled quinone (Q) molecule and FMN are displayed with atomic coloring (carbon – cyan, oxygen – red and nitrogen - blue) and FeS clusters as yellow and pink spheres. The thicker blue and black arrows indicate the direction of the electron transfer and proton pumping, respectively. The two dashed boxes highlight the coupling region and the Nqo12 subunit, which are shown in more details in panels B and C, respectively. (B) The highly conserved charged and polar amino acid residues form a connection between the Q reduction site near Tyr87 (Nqo4) and the middle of the membrane domain. (C) Highly conserved amino acid residues that are present in Nqo12 subunit and not in Nqo13/14 subunits are marked in red. (D) Multiple sequence alignment of Nqo12/13/14 subunits from different organisms (*T.t.* – *Thermus thermophilus*, *E.c.* – *Escherichia coli*, *H.s.* – *Homo sapiens*, *Y.l.* – *Yarrowia lipolytica*). The residues shown in bold are those that are central to Nqo12 function (circled in panel C, see main text).

hydrophobic methionines in Nqo12. The functional relevance of these distinct differences remains unclear, despite overall structural homology between the three antiporter-like subunits. It is possible that this aberration is associated with the dual role of Nqo12 subunit, in efficiently coupling the proton pumping, being the most distant subunit from the "active site" of redox reactions (Q-tunnel), and also to act as the subunit responsible for termination or reverse of the 'electrostatic/conformation signal' from the Q redox site near N2 [5]. Here, we focus on the Nqo12 subunit, and by using multiscale computational methods trace the proton transfer path in full molecular details, through which protons are translocated from the N-side to the P-side of the membrane. Based on extensive set of simulations, we identify novel functional elements in Nqo12 subunit that enables the enzyme to achieve tight coupling between Q redox reactions and proton pumping.

2. Computational methods

2.1. Classical molecular dynamics simulations

We performed atomistic classical molecular dynamics (MD) simulations on bacterial complex I from *Thermus thermophilus* (PDBid 4HEA) [7] using large (L) and small (S) model systems. The large model systems comprise the entire bacterial complex I embedded in pure POPC (1-palmitoyl-2-oleoylphosphatidylcholine) membrane, whereas the smaller systems, containing only subunits Nqo12/13/14 in POPC membrane, were constructed to enhance sampling of some of the modeled states. Truncation of model systems to enhance sampling may lead to artifacts. However, earlier us and others have successfully performed simulations on small model systems and validated the findings based on large model systems [14–16]. For both L and S setups, we used the Orientations of Protein in Membrane (OPM) database [17] to correctly position the enzyme into the membrane. The missing parts of the protein were modeled as in earlier works [10,18]. The protein-membrane systems were embedded in TIP3 water molecules with 0.1 M Na^+/Cl^- ions mimicking the physiological salt concentration. The S and L model systems consist of approximately 180,000 and 850,000 atoms, respectively. Several classical MD simulations in different protonation/conformational states were performed including additional replicas, as described in Table S1.

We used software GROMACS [19] with CHARMM forcefield for protein, lipids, solvent and ions [20–22] to perform the classical MD simulations. CHARMM force field parameters for reduced iron sulphur clusters and FMN were used as described earlier [10,18]. We energy minimized the initial models to remove possible atomic clashes, and performed 100 ps NVT and 1 ns NPT equilibrations to stabilize the pressure and temperature of the system to physiological 1 atm and 310 K, respectively. For the purpose, Parrinnello-Rahman barostat [23,24] and Nose-Hoover thermostat [25,26] were used. A 2 fs timestep was achieved by using the LINCS algorithm [27], which constrains the covalent bonds between hydrogens and other non-hydrogen atoms. PME [28], as implemented in GROMACS, was used to calculate the long range electrostatics. The simulation trajectories were analyzed with the visualization software VMD [29]. The software PropKa [30] was used to measure the pK_a values on simulation snapshots. The time series plots are shown as a running average of 20 nanoseconds (20 simulation snapshots) with real data in light grey color.

2.2. Hybrid quantum mechanical/molecular mechanical (QM/MM) simulations

In order to study the transfer of protons through the classically identified hydrated paths, we performed hybrid QM/MM MD simulations on different regions of the Nqo12 subunit (Table S2 and Fig. S1). The QM/MM simulations were performed with QCHEM/CHARMM [31,32] software using the additive electrostatic coupling. The MM region consisted of the hydrated subunits Nqo12/13/14, whereas the QM region comprised selected residues and water molecules (see Table S2). The boundary between QM and MM regions was treated with the link atom formalism, in which a dummy atom was introduced between the Cα and Cβ of amino acid residues of interest. A 1000 step classical energy minimization was performed followed by a 200 step QM/MM energy minimization, prior to the launch of MD in QM/MM framework. These simulations, including replicas, were performed with B3LYP [33–35] density functional, 6-31G* or 6-311G* basis set (as implemented in QCHEM [31]) and by using the dispersion corrections [36] at 310 K with 1 fs time step.

3. Results

3.1. Proton transfer pathway in the Nqo12 subunit

We performed a ~2 μs MD simulation (setup 1, see Table S1) on a large model system of bacterial complex I from *Thermus thermophilus* and identified two regions where water molecules enter from the N-side of the membrane in Nqo12 subunit (regions A and B in Fig. 2). These two hydrated regions have been observed earlier in simulation studies [10,13]. However, explicit proton transfer through conserved amino acids and water molecules, and potential crosstalk between the two regions remain unclear, which is necessary to understand the key role of distal Nqo12 subunit. Here, we study both these regions by multiscale computer simulations and identify novel aspects of Nqo12 subunit that are important to achieve long-range electron-protein coupling in complex I.

Region A is formed by helices 8 and 11, and the other region (B) by helices 5–7 around a highly conserved residue Ser138 found in Nqo12, but not in Nqo13/14. We find that the hydrated region A forms a potential proton uptake route in the Nqo12 subunit (Fig. 2) and the protonated Lys329, which is unique to Nqo12 subunit, H-bonds with the neutral His325 (Fig. 3A and C) (see also Table S3 and Fig. S2). A second

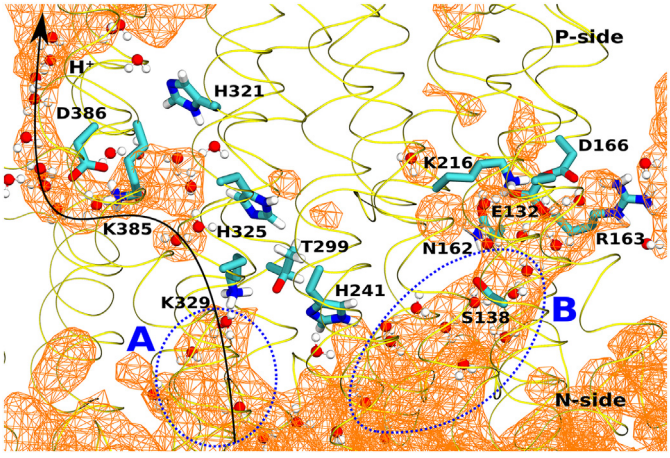

Fig. 2. Water occupancy in the Nqo12 subunit shown as an orange colored mesh at 0.2 isovalue (20% occupancy). The two hydrated regions (A and B) are highlighted by blue dotted lines together with a putative proton transfer route (solid black line). The residues shown are highly conserved in the Nqo12 antiporter-like subunit across various species. The data presented is from setup 5 (Table S1).

conformation of protonated Lys329 is also observed in our simulations in which it points close to the N-side of the membrane ("down" conformation, 5–7 Å away from His325, Fig. 3B and C). In this latter arrangement, Lys329 forms a water-based connection to the N-side of the membrane (Fig. 3B and C), also involving the highly conserved Lys292. Remarkably, the connectivity between the protonated Lys329 and the N-side of the membrane as well as the hydration around His325/Lys329 pair is entirely lost upon H-bonding with His325 (Figs. 3). In order to further explore this issue, we performed additional MD simulations (Table S1) in which protonation states of Lys329 and His325 were altered systematically. We find that when Lys329 is neutral, and His325 protonated (setup 2 in Table S1), the H-bond between the two remains stable and water occupancy below Lys329 does not increase (Figs. 3C and S2). Only when both Lys329 and His325 are modeled neutral (setup 3, Table S1) the H-bond between the two is unstable and sidechain of Lys329 explores a number of arrangements including predominant "down" conformation (Fig. 3C). Continuum electrostatic calculations show His325 has a low pKa (< 4), thus favoring its neutral protonation state. However, Lys329 shows conformation-dependent pKa changes, with an "up shifted" pKa (by 1–2 pK units) in its "down" conformation (pKa ~ 8) in contrast to "up" conformation when it H-bonds to His325 (pKa ~ 6), that is away from the N-side of the membrane. Overall, these data point out that Lys329, a potential proton uptake residue for Nqo12 proton channel, preferentially points to the N-side of the membrane when modeled in its neutral state (together with neutral His325, see Fig. 3), whereas, when modeled in protonated state stabilizes an "up" conformation. The "high-to-low" pKa shift coupled with "down-to-up" dynamics of Lys329 suggest that only after the proton has been transferred from it towards the P-side, it flips to the "down" conformation to uptake another proton.

In order to shed light on the explicit proton transfer that may take place via Lys329, we performed hybrid quantum mechanical/molecular mechanical (QM/MM) MD simulations (setup Q1 in Table S2) and observed rapid protonation of the neutral Lys329 in its "down" conformation in multiple independent simulations (Fig. S1 and Video S1), which is in agreement with the pKa calculations that show higher proton affinity relative to "up" conformation (see below). Overall, the transfer of a proton to Lys329 from the N medium and its protonation-state dependent dynamics supports its role in proton uptake and transfer, and is also in excellent agreement with the site directed mutagenesis data that show a drastic drop in Q reductase activity (11% of wild type) [37] upon mutation of homologous lysine to alanine in *E. coli* complex I.

We next analyzed the proton transfer pathway from Lys329 towards the P side of the membrane. The region comprises two conserved histidines (His321 and His325), a few other polar residues and water molecules that diffused in to this region upon dynamics (Figs. 1 and 2). Site-directed mutagenesis data on complex I from *E. coli* suggests that the two histidines are not critical for the catalytic activity of the enzyme [38]. The path from the central region continues towards a highly conserved and functionally critical Lys385, which has charged counterparts in Nqo13 (Glu377) and Nqo14 (Lys345) subunits. We observed that the sidechain of Lys385 is dynamic and it hydrogen bonds to His321 (Fig. 3E and F); a scenario also observed in crystal and electron microscopy-based structures (Table S3), thereby consolidating dynamical findings from simulations. In order to further clarify how a proton transfer would occur beyond Lys329, the putative proton uptake site, we performed QM/MM simulations and observed spontaneous protonation of Lys385 from a hydronium or Lys329, by passing His321/325, in a number of independent simulations (setup Q2 in Table S2; see Fig. S1 and Video S2), which is also in agreement with the lower pKa of Lys329 predicted by approximate continuum electrostatics based approach. Biochemical characterization of corresponding lysine (Lys385) in *E. coli* enzyme shows that the residue is important for maintaining the enzyme architecture as well as its activity, and our multiscale simulations are also in accord with this notion [37,38]. Moreover, given

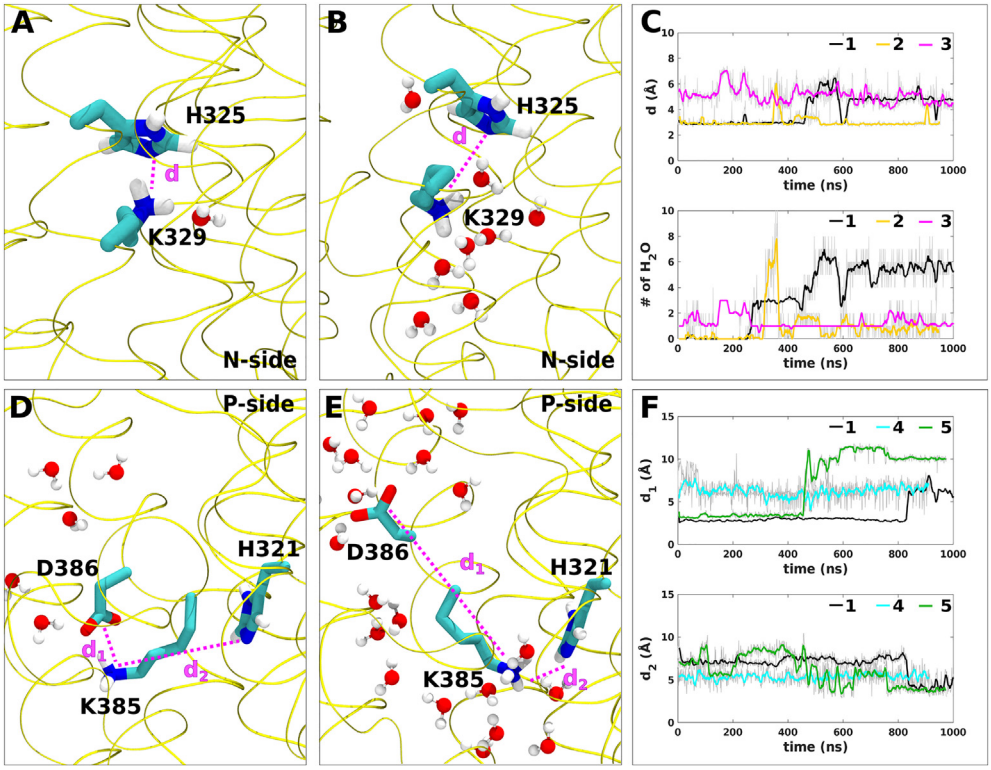

Fig. 3. Hydration-dehydration coupled to protein dynamics in Nqo12 subunit. (A) The "up" conformation of protonated Lys329 in H-bonding with His325 precludes water-based connectivity to the N-side of the membrane. (B) Lys329 in its "down" conformation pointing away from His325 forms hydrated paths towards the N-side of the membrane. (C) Simulation data (setups 1, 2 and 3 in black, orange and magenta, respectively) show increase in hydration within 5 Å of Lys329 upon its flip from "up" (d ~ 3 Å) to "down" (d ~ 6 Å) conformation. (D-F) Dynamics of conserved Asp386/Lys385 pair of Nqo12 subunit. Anionic Asp386 and protonated Lys385 forms an ion-pair (panel D, d_1 ~ 3 Å and d_2 ~ 6–7 Å). A second conformation of Lys385, in which it H-bonds with His321, is shown in panel E (d_1 ~ 7–10 Å and d_2 ~ 3–4 Å), whereas Asp386 moves to its crystallographic conformation (see also main text). (F) The top panel shows the distance (d_1) between Lys385 and Asp386, and bottom panel shows the distance (d_2) between Lys385 and His321 in different simulation setups (setups 1, 4 and 5 in black, cyan and green, respectively) demonstrating the conformational variation of Lys329 and Asp386. Distances (d, d_1 and d_2) are plotted using atoms NE2 (His325 and His321), NZ (Lys329) and CG (Asp386) and are shown with dotted lines in panels A and B (setup 1) and D and E (setup 5).

that a direct proton transfer occurs from Lys329 to Lys385, by passing His321/325, is congruent with the minor effect these histidines cause to catalytic activity upon mutation. However, they likely play an important role in stabilization of water molecules and amino acid residues in the proton channel.

The residue adjacent to Lys385 is a highly conserved acidic residue Asp386 (Fig. 2), which showed decreased proton pumping efficiency upon mutation to Ala in complex I from *E. coli* [38], suggesting its important role in proton translocation. Due to the charged states simulated for both Lys385 and Asp386, the salt-bridge between them rapidly formed (Fig. 3D). This interaction remained stable in our long-time scale simulations (Fig. S2), and when QM/MM simulations were performed on this region, the proton is indeed found to stabilize in a shared fashion between the two residues (setup Q3 in Table S2). Based on this, we simulated an additional state (setup 4 in Table S1) by modeling both residues in their charge neutral states and observed stabilization of Lys385 in its crystallographic conformation (Fig. 3E and Table S3). In another simulation setup (#5), which is similar to setup 1 (Table S1), Asp386 is also found to stabilize in a conformation that is similar to its crystallographic arrangement, and may represent its proton releasing mode towards the P side of the membrane (Fig. 3E). Out of several independent QM/MM simulations (Table S2), deprotonation of Asp386 is rarely observed (Fig. S1), which is in part due to limited simulation sampling during QM/MM dynamics. Indeed, when a proton is modeled as a hydronium ion next to deprotonated Asp386, it rapidly stabilizes on the water cluster instead of Asp386, suggesting the existence of an energy barrier towards protonation of Asp386.

Overall, by combining classical and QM/MM modeling approaches we have traced a putative proton transfer path in the Nqo12 subunit to full atomic details. It consists of a proton uptake site in the form of a highly dynamic residue Lys329, and a proton releasing machinery comprising conformationally flexible Lys385/Asp386 pair. It is the protonation-state and hydration-state coupled dynamics of these charged residues that is central to proton pumping in the most distant antiporter-like subunit of complex I.

3.2. Dynamics of His241 and protonation-coupled hydration

We find another region in the Nqo12 subunit that rapidly (~200 ns) fills with water molecules (region B in Fig. 2) and is adjacent to the proton transfer route identified above (region A, Fig. 2). A number of highly conserved residues surround this small hydrated pocket that includes His241, Asn162, Ser138, and the conserved K/E pair (Lys217/Glu132) of the Nqo12 subunit. Among these, His241 resides in the broken segment of TM helix 8 with no analogous counterpart in Nqo13/14. Interestingly, it occupies a position one turn below the canonical position of conserved lysines (Lys235 and Lys216 of Nqo13 and Nqo14, respectively, see Fig. 1D) that have been suggested to participate in proton uptake from the N side of the membrane. Earlier, based on this analogy, His241 has also been implicated in proton transfer [39,40]. Our classical simulations reveal that His241 is highly mobile and a number of its conformations are populated, including the one in which it is proximal to Lys329 and another one in which it is closer to Ser138 (Fig. 4). Interestingly, the latter arrangement is in part supported by the structural data, where analogous histidine is next to the conserved serine (see Table S3). We find that His241 approaches Lys329 (region III in Fig. 4C) when either Lys329 or His241 is modeled protonated (setups 6, 7 and 8 in Table S1). In contrast, when Lys329 is modeled neutral and His325 protonated (setups 2 and 10 in Table S1), His241 diffuses away and participates in hydrogen bonding with Ser138 (region I in Fig. 4C). This data, from multiple independent simulations, suggests that the observed dynamics of His241 is coupled to the protonation state of residues identified in the proton channel (Lys329 and His325). We note that a histidine residue analogous to His241 is uniquely conserved in the MrpA subunit (not in MrpD), and functional role of this residue and the surrounding region in Na^+ transport has

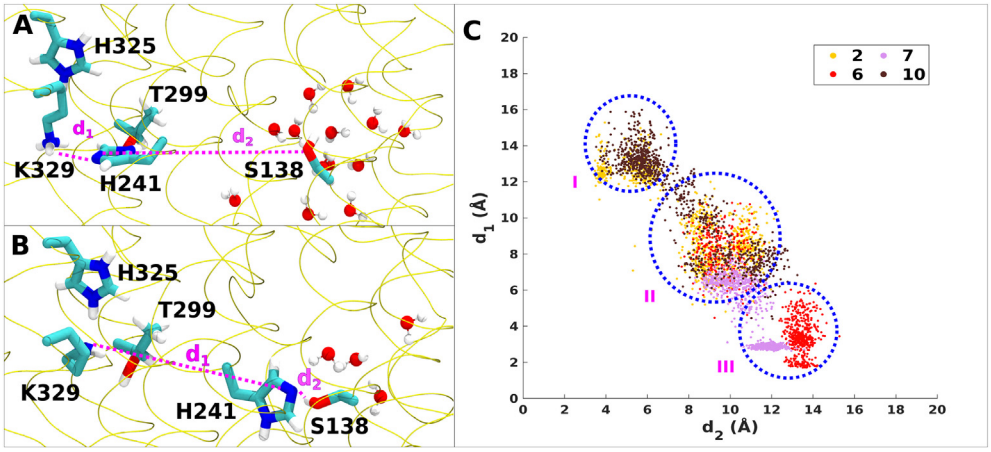

Fig. 4. Conformational dynamics of conserved His241 in Nqo12 subunit. (A) His241 approaches to the putative proton uptake site Lys329 (A) and moves towards conserved Ser138 (B) coupled with the changes in hydration in region B (see also Fig. 2). (C) A scatter plot revealing the conformational diversity of His241 across several simulation setups (Table S1). Distance d_1 is between atoms NE2 (His241) and NZ (Lys329), and distance d_2 between atoms NE2 (His241) and OG (S138) (see also Table S3). Panels A and B are prepared from setups 6 and 2, respectively (Table S1).

earlier been investigated [41]. The significant hydration observed in our simulations in the domain between His241 and Ser138 (region B, Fig. 2) as well as protonation dependent dynamics of His241 allows us to speculate that this region is also crucial for the function of complex I (see Discussion).

3.3. Salt-bridge dynamics coupled to hydration

All three antiporter-like subunits consist of a conserved Lys/Glu (K/E) pair that has been suggested to participate in coupling the long range redox-coupled proton pumping in complex I based on structural [7,42] and computational [10,13] approaches (Fig. 1). In the Nqo12 subunit, the two residues Lys216 and Glu132 (K/E pair) rapidly form a salt bridge in their charged states (setup 1), which remains stable in simulations (Figs. 5 and S2). Interestingly, this salt bridge is accessible to the N-side of the membrane via the hydrated region B identified above (Fig. 2). Note that a similar hydrated path does not form in the two other antiporter-like subunits Nqo13 and Nqo14 (Fig. S3), suggesting clear differences in the architecture of antiporter-like subunits Nqo12 and Nqo13/14. When we performed a QM/MM simulation by modeling an explicit proton (H_3O^+) near the N-side of the membrane (setup Q5 in Table S2), it rapidly diffused through the water molecules in the hydrated region B leading to the protonation of Glu132 (a modeled Na^+ ion also diffused (setup 18 in Table S1), Fig. S4). Remarkably, the hydration in region B is found to be strongly coupled to the protonation state and stability of salt bridge between Lys216 and Glu132; upon protonation of Glu132, the pair remains dissociated, coupled to the dehydration of region B (Fig. 5). This effect is observed in multiple independent classical MD simulations (setups 11, 12 and 14 in Table S1), and also with the protonation of Glu166 (setup 15 in Table S1), a conserved residue spatially adjacent to Glu132. We also find transient events in which K/E pair opens despite simulated in its charged form and that is found to be correlated with partial dehydration of region B (Fig. S5, see also Fig. 5). Interestingly, the dissociation of K/E pair causes the anionic Glu132 to change its conformation, while the protonated Lys216 remains approximately in its original location. This results in formation of a charged-network between Glu132-Arg163 of Nqo12 and Glu377 of Nqo13, which may represent the second stable arrangement of Glu132, as also observed earlier [10,13].

Overall, we find that the dynamics of K/E pair in Nqo12 subunit is coupled to the hydration/dehydration observed in region B (Fig. 5). However, a question is raised that what drives the 'open/closed'

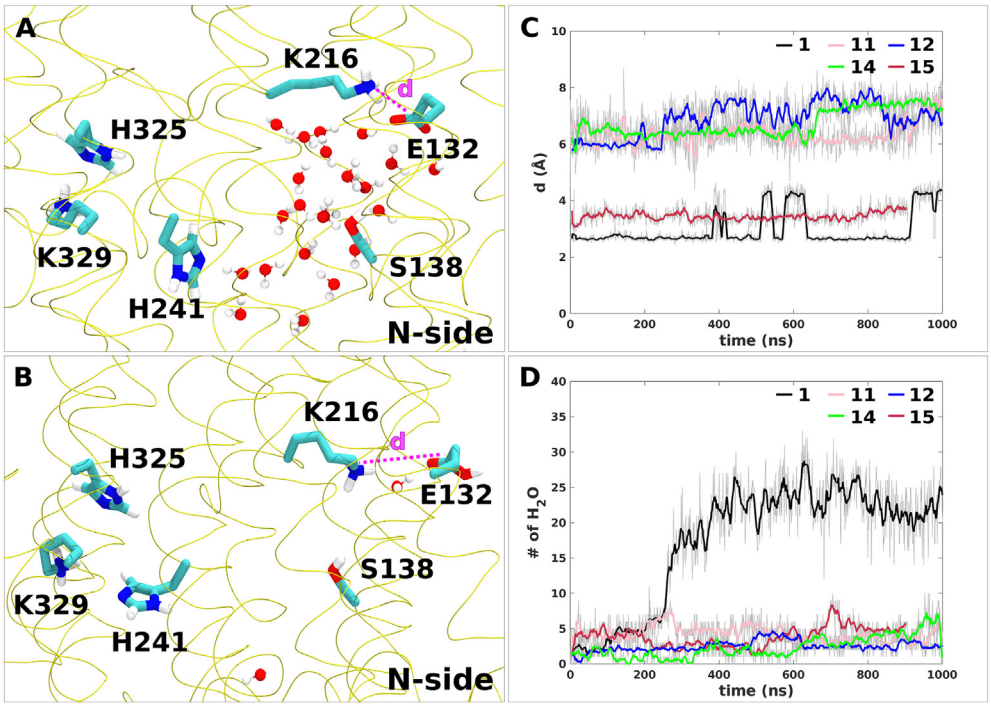

Fig. 5. Dynamics of conserved Lys-Glu ion pair and coupled hydration in region B (A) Ion pair between Lys216 and Glu132 is "closed", when Glu132 is deprotonated and region B remains hydrated (snapshot from setup 1). (B) Ion pair between Lys216 and Glu132 is "open" upon charge neutralization of Glu132, leading to lower water occupancy in region B (snapshot from setup 12). (C) The distance between NZ (K216) and CD (Glu132) atoms is plotted from several simulations. (D) Number of water molecules within 8 Å of Ser138 in same set of simulations. The data from simulation setups 1, 11, 12, 14 and 15 are shown in black, pink, blue, green and maroon colors, respectively.

transitions of the K/E ion-pair in the Nqo12 subunit, which may be necessary to drive proton pumping in complex I [11,12]. We find that there are two such possibilities; either by neutralizing Glu132 or by stabilizing its alternative conformation via interaction to Arg163 (to Glu377 of Nqo13). In either case, the observed dehydration of region B is likely to have a functional role (see Discussion).

In contrast to the local coupling between hydration in region B and K/E pair dynamics, we did not find consistent changes in hydration in region A (proton uptake route) with the corresponding changes in "open/closed" dynamics of K/E pair, which is likely due to much longer distance between the two regions (~20 Å).

4. Discussion

A number of molecular mechanisms have been proposed on how complex I may drive proton pumping (see refs. in [11]). Notably, computational approaches such as MD simulations, continuum electrostatics and quantum chemical calculations have been pivotal in providing detailed molecular insights [11,12]. One remarkable mechanistic suggestion on how electrostatic coupling between the central lysine residues and the K/E pair may be achieved is given by Kaila and colleagues [12,13], who observed based on free energy calculations that the dissociation of Nqo13 K/E pair is energetically favorable when the lysine involved in proton uptake from the N medium is modeled neutral. This electrostatic (and/or conformational) coupling between charged residues could be of central importance in proton pumping by complex I, as alluded earlier [5]. However, in the terminal Nqo12 subunit lysine residue (Lys329) is ca. 20 Å from the K/E pair, which is about 8–10 Å longer than what is observed in Nqo13/14 subunits, and which would render the electrostatic coupling between these charged residues very weak. Therefore, it remains unclear how proton pumping is achieved in the Nqo12 subunit, which is at a maximal distance from the site of Q redox reactions. Our simulation data reveal that there are unique structural and functional features present in the Nqo12 subunit that may compensate for this deficit.

First, we find that a rapid Grotthuss-like proton transfer occurs from the N phase of the membrane to the "down flipped" Lys329 through a chain of 3–4 water molecules. The distance of Lys329 from the N medium is 4–5 Å shorter than the distance between central Lys residues of the Nqo13/14 subunits and the N phase. This short distance together with the recruitment of fewer water molecules may provide kinetic enhancement in proton uptake by the distal Nqo12 subunit, where the effect of Q redox activity is expected to be minimal due to large distance (ca. 200 Å). Second, our simulation data show that upon protonation Lys329 stabilizes an "up flipped" conformation by hydrogen bonding to His325, which reduces the hydration between the N phase of the membrane and lysine. We propose that this protonation-state coupled dynamics of Lys329 and associated dehydration are crucial to prevent the thermodynamically favorable back-flow of protons to the N-side of the membrane, arguing for a potential 'valve' role of conserved Lys329.

Due to longer distance (~20 Å) between the K/E pair and proton uptake site Lys329, the electrostatic coupling between them is likely to be weaker by a factor of half in the Nqo12 subunit (ca. 4 kcal/mol weaker in Nqo12 compared to Nqo13/14) (see also [13]). However, this may be compensated by the shorter distance (ca. 11 Å), and hence stronger coupling with the proton releasing lysine (Lys385); note that the analogous distance between similar residues in Nqo13/14 is much larger (~ 18 Å). Therefore, we argue that the unique location of Lys329 in the Nqo12 subunit (closer to the N phase and to Lys385), consequently a shorter proton transfer path, is to efficiently couple the translocation of protons with Q redox chemistry in the Q tunnel.

The Nqo12 K/E pair is ca. 130 Å from the Q tunnel in contrast to the K/E pairs of Nqo13/14, which are at a distance of ca. 80/40 Å, respectively. This is expected to make the electrostatic/conformational coupling weaker, and therefore, additional molecular mechanisms are necessary to efficiently couple the translocation of protons in the most distant Nqo12 subunit. Our simulation data suggests that the alternative position of His241, in H-bonding with Ser138 (both residues unique to Nqo12, see also Fig. S6), and/or partial proton transfer from the N phase (or protonated His241) to Glu132, stabilizes the "open" conformation of the K/E pair, which is necessary to drive proton transfer forward from Lys329 to Lys385. Once the proton is transferred to Lys385 and is ready to be released towards the P-side, one can envisage a transient state in which the entire cascade of reactions may run backwards, leading to loss of proton pumping and efficiency. We propose that the acidic residue adjacent to Lys385, that is Asp386, which is uniquely present in the Nqo12 subunit, plays a central role in preventing this loss of energy by extracting and transferring protons from Lys385 to the P-side of the membrane. It is possible that the release of the first proton to the P-side of the membrane (from Asp386 of Nqo12) is a necessary trigger that leads to sequential proton pumping by Nqo13 and Nqo14 (in that order) during the 'reverse wave' of electrostatic polarization and conformational changes [5,12].

Nqo12 subunit shares similarity with the MrpA subunit, whereas Nqo13/14 are more similar to MrpD. Our simulations identified a region in the Nqo12 subunit that hydrates sufficiently to create a potential path for the transfer of charged ions. Remarkably, some of the amino acid residues found in this region are also conserved in the MrpA subunit, which suggests a potentially shared functional role of this region in Mrp antiporters and complex I. We speculate that in MrpA subunit the Na^+/H^+ antiporter function is achieved by the translocation of ion via hydrated region B coupled to the transfer of proton in opposite direction through region A identified in this work, supporting similar coupling principles across different bioenergetic enzymes.

5. Conclusions

Long range coupling between electron and proton is central to photosynthetic and respiratory enzymes involved in biological energy transduction. However, the factors that govern these charge transfers are poorly understood because of current limitations in experimental technology. Here, we apply multiscale computational approaches to study such effects in respiratory complex I, an enzyme of primary importance in energy generation and mitochondrial function. Our results highlight that the protonation-state dependent conformational dynamics of amino acid residues in Nqo12 subunit and coupled hydration/dehydration effects are central elements responsible for efficiency and directionality of proton pumping in complex I.

Supplementary data to this article can be found online at https://doi.org/10.1016/j.bbabio.2020.148185.

Acknowledgements

VS acknowledges research funding from the Academy of Finland, the Sigrid Jusélius Foundation and the University of Helsinki and helpful discussion with Prof. Mårten Wikström and Prof. Volker Zickermann. OH is supported by the doctoral program in chemistry and molecular sciences (CHEMS) of the University of Helsinki. We thank the Center for Scientific Computing, Finland for generous computational support including *Grand Challenge* resources (project - cIDYNA).

Declaration of competing interest

The authors declare that they have no known competing financial interests or personal relationships that could have appeared to influence the work reported in this paper.

References

[1] L.A. Sazanov, A giant molecular proton pump: structure and mechanism of respiratory complex I, Nat. Rev. Mol. Cell Biol. 16 (2015) 375–388.
[2] A.-N.A. Agip, J.N. Blaza, J.G. Fedor, J. Hirst, Mammalian respiratory complex I

through the lens of cryo-EM, Annu. Rev. Biophys. 48 (2019) 165–184.
[3] C. Wirth, U. Brandt, C. Hunte, V. Zickermann, Structure and function of mitochondrial complex I, Biochimica Et Biophysica Acta (BBA)-Bioenergetics, 1857 (2016) 902–914.
[4] U. Brandt, A two-state stabilization-change mechanism for proton-pumping complex I, Biochimica et Biophysica Acta (BBA)-Bioenergetics, 1807 (2011) 1364–1369.
[5] L. Euro, G. Belevich, M.I. Verkhovsky, M. Wikström, M. Verkhovskaya, Conserved lysine residues of the membrane subunit NuoM are involved in energy conversion by the proton-pumping NADH: ubiquinone oxidoreductase (Complex I), Biochimica et Biophysica Acta (BBA)-Bioenergetics, 1777 (2008) 1166–1172.
[6] R.G. Efremov, L.A. Sazanov, The coupling mechanism of respiratory complex I—a structural and evolutionary perspective, Biochimica et Biophysica Acta (BBA)-Bioenergetics, 1817 (2012) 1785-1795.
[7] R. Baradaran, J.M. Berrisford, G.S. Minhas, L.A. Sazanov, Crystal structure of the entire respiratory complex I, Nature 494 (2013) 443–448.
[8] V. Zickermann, C. Wirth, H. Nasiri, K. Siegmund, H. Schwalbe, C. Hunte, U. Brandt, Mechanistic insight from the crystal structure of mitochondrial complex I, Science 347 (2015) 44–49.
[9] N. Agmon, The grotthuss mechanism, Chem. Phys. Lett. 244 (1995) 456–462.
[10] O. Haapanen, V. Sharma, Role of water and protein dynamics in proton pumping by respiratory complex I, Sci. Rep. 7 (2017) 7747.
[11] O. Haapanen, V. Sharma, A modeling and simulation perspective on the mechanism and function of respiratory complex I, Biochimica et Biophysica Acta (BBA)-Bioenergetics, (2018).
[12] V.R. Kaila, Long-range proton-coupled electron transfer in biological energy conversion: towards mechanistic understanding of respiratory complex I, J. R. Soc. Interface 15 (2018) 20170916.
[13] A. Di Luca, A.P. Gamiz-Hernandez, V.R. Kaila, Symmetry-related proton transfer pathways in respiratory complex I, Proc. Natl. Acad. Sci. 114 (2017) E6314–E6321.
[14] P. Tan, Z. Feng, L. Zhang, T. Hou, Y. Li, The mechanism of proton translocation in respiratory complex I from molecular dynamics, Journal of Receptors and Signal Transduction 35 (2015) 170–179.
[15] V.R. Kaila, M. Wikström, G. Hummer, Electrostatics, hydration, and proton transfer dynamics in the membrane domain of respiratory complex I, Proc. Natl. Acad. Sci. 111 (2014) 6988–6993.
[16] O. Haapanen, A. Djurabekova, V. Sharma, Role of second quinone binding site in proton pumping by respiratory complex I, Frontiers in Chemistry 7 (2019) 221.
[17] M.A. Lomize, I.D. Pogozheva, H. Joo, H.I. Mosberg, A.L. Lomize, OPM database and PPM web server: resources for positioning of proteins in membranes, Nucleic Acids Res. 40 (2011) D370–D376.
[18] V. Sharma, G. Belevich, A.P. Gamiz-Hernandez, T. Róg, I. Vattulainen, M.L. Verkhovskaya, M. Wikström, G. Hummer, V.R. Kaila, Redox-induced activation of the proton pump in the respiratory complex I, Proc. Natl. Acad. Sci. 112 (2015) 11571–11576.
[19] M.J. Abraham, T. Murtola, R. Schulz, S. Páll, J.C. Smith, B. Hess, E. Lindahl, GROMACS: high performance molecular simulations through multi-level parallelism from laptops to supercomputers, SoftwareX 1 (2015) 19–25.
[20] A.D. MacKerell Jr., D. Bashford, M. Bellott, R.L. Dunbrack Jr., J.D. Evanseck, M.J. Field, S. Fischer, J. Gao, H. Guo, S. Ha, All-atom empirical potential for molecular modeling and dynamics studies of proteins, J. Phys. Chem. B 102 (1998) 3586–3616.
[21] A.D. MacKerell, M. Feig, C.L. Brooks, Extending the treatment of backbone energetics in protein force fields: limitations of gas-phase quantum mechanics in reproducing protein conformational distributions in molecular dynamics simulations, J. Comput. Chem. 25 (2004) 1400–1415.
[22] J.B. Klauda, R.M. Venable, J.A. Freites, J.W. O'Connor, D.J. Tobias, C. Mondragon-Ramirez, I. Vorobyov, A.D. MacKerell Jr., R.W. Pastor, Update of the CHARMM all-atom additive force field for lipids: validation on six lipid types, J. Phys. Chem. B 114 (2010) 7830–7843.
[23] M. Parrinello, A. Rahman, Crystal structure and pair potentials: a molecular-dynamics study, Phys. Rev. Lett. 45 (1980) 1196.
[24] M. Parrinello, A. Rahman, Polymorphic transitions in single crystals: a new molecular dynamics method, J. Appl. Phys. 52 (1981) 7182–7190.
[25] S. Nosé, A unified formulation of the constant temperature molecular dynamics methods, J. Chem. Phys. 81 (1984) 511–519.
[26] W.G. Hoover, Canonical dynamics: equilibrium phase-space distributions, Phys. Rev. A 31 (1985) 1695.
[27] B. Hess, P-LINCS: a parallel linear constraint solver for molecular simulation, J. Chem. Theory Comput. 4 (2008) 116–122.
[28] T. Darden, D. York, L. Pedersen, Particle mesh Ewald: an N· log (N) method for Ewald sums in large systems, J. Chem. Phys. 98 (1993) 10089–10092.
[29] W. Humphrey, A. Dalke, K. Schulten, VMD: visual molecular dynamics, J. Mol. Graph. 14 (1996) 33–38.
[30] M.H. Olsson, C.R. Søndergaard, M. Rostkowski, J.H. Jensen, PROPKA3: consistent treatment of internal and surface residues in empirical p K a predictions, J. Chem. Theory Comput. 7 (2011) 525–537.
[31] Y. Shao, Z. Gan, E. Epifanovsky, A.T. Gilbert, M. Wormit, J. Kussmann, A.W. Lange, A. Behn, J. Deng, X. Feng, Advances in molecular quantum chemistry contained in the Q-Chem 4 program package, Mol. Phys. 113 (2015) 184–215.
[32] B.R. Brooks, C.L. Brooks III, A.D. Mackerell Jr., L. Nilsson, R.J. Petrella, B. Roux, Y. Won, G. Archontis, C. Bartels, S. Boresch, CHARMM: the biomolecular simulation program, J. Comput. Chem. 30 (2009) 1545–1614.
[33] A.D. Becke, Density-functional exchange-energy approximation with correct asymptotic behavior, Phys. Rev. A 38 (1988) 3098.
[34] A.D. Becke, Density-functional thermochemistry. III. The role of exact exchange, J. Chem. Phys. 98 (1993) 5648–5652.
[35] C. Lee, W. Yang, R.G. Parr, Development of the Colle-Salvetti correlation-energy formula into a functional of the electron density, Phys. Rev. B 37 (1988) 785.
[36] S. Grimme, J. Antony, S. Ehrlich, H. Krieg, A consistent and accurate ab initio parametrization of density functional dispersion correction (DFT-D) for the 94 elements H-Pu, J. Chem. Phys. 132 (2010) 154104.
[37] M. Sato, P.K. Sinha, J. Torres-Bacete, A. Matsuno-Yagi, T. Yagi, Energy transducing roles of antiporter-like subunits in Escherichia coli NDH-1 with main focus on subunit NuoN (ND2), J. Biol. Chem. 288 (2013) 24705–24716.
[38] E. Nakamaru-Ogiso, M.-C. Kao, H. Chen, S.C. Sinha, T. Yagi, T. Ohnishi, The membrane subunit NuoL (ND5) is involved in the indirect proton pumping mechanism of Escherichia coli complex I, J. Biol. Chem. 285 (2010) 39070–39078.
[39] J. Hirst, Mitochondrial complex I, Annu. Rev. Biochem. 82 (2013) 551–575.
[40] L.A. Sazanov, The mechanism of coupling between electron transfer and proton translocation in respiratory complex I, J. Bioenerg. Biomembr. 46 (2014) 247–253.
[41] E. Sperling, K. Górecki, T. Drakenberg, C. Hägerhäll, Functional differentiation of antiporter-like polypeptides in complex I; a site-directed mutagenesis study of residues conserved in MrpA and NuoL but not in MrpD, NuoM, and NuoN, PLoS One 11 (2016) e0158972.
[42] R.G. Efremov, L.A. Sazanov, Structure of the membrane domain of respiratory complex I, Nature 476 (2011) 414–420.